SURFACE DEFORMATION INVESTIGATED WITH SBAS-DINSAR APPROACH BASED ON PRIOR KNOWLEDGE

HUANG Qi-huan [a], *, HE Xiu-feng [a]

[a] Institute of Satellite Navigation & Spatial Information System, Hohai University, Nanjing, P. R. China – (InSAR, xfhe)@hhu.edu.cn

Commission Ⅲ, WG I/2

ABSTRACT:

Although Differential Synthetic Aperture Radar Interferometry (DInSAR) has been successfully used for deformation mapping, it is easily suffered from both spatial and temporal decorrelation which limits its application, especially for long-term deformation mapping. Based on the DInSAR algorithm, Small BAseline Subset (SBAS) approach, which generates interferograms only between two SAR images with small spatial baseline, can reduce both spatial and temporal decorrelation using a data set of SAR images acquired subsequently. SBAS-DInSAR approach allows us to generate mean deformation velocity maps and displacement time series. In this paper, the surface deformation of the Nanjing City, P. R. China was investigated with SBAS-DInSAR approach. In particular, a cubic behaviour for the time variation of the deformation phase signal was assumed as prior knowledge for the investigated area, and the deformation parameters obtained in an optimal least square(LS) way directly, simplify the SBAS algorithm which linking the interferograms using Singular value decomposition (SVD) method. Results of 13 differential interferograms generated by 8 SAR images in Nanjing from August 1996 to April 2000, demonstrate its efficiency.

1. INTRODUCTION

Differential Synthetic Aperture Radar Interferometry (DInSAR) is a relatively new technique that has been successfully used for generating large-scale surface deformation maps on a dense grid and with a centimetre to millimetre accuracy (C. Prati, 1992), within several ten years development, the interest of the scientific community about DInSAR approach is now progressively moving from the study of a single deformation episode to the temporal evolution of the detected deformations.
t
ion of temporal and spatial decorrelation as well as atmospheric inhomogeneous which limit its accuracy for deformation detection; CR approach uses man-made feature called Corner Reflector to overcome the decorrelation phenomena at the expense of cost,

therefore ,the most disadvantage of CR approach is its only showing pointwise information; The PS approach maximizes the number of the acquisitions used ,generates DInSAR interferograms, for each available acquisition even if the exploited data pair is characterized by a large baseline (even larger than the critical baseline), with respect to a common (master) image, and, therefore, affected by baseline decorrelation phenomena. It is evident that, in this case, the use of all the available data acquisitions is accomplished, but at the expense of imaged pixel density; indeed, only those targets that exhibit sufficiently high coherence values are considered, and their density may be in some cases rather low; this often happens, for instance, in nourban areas.

Small BAseline Subset (SBAS) approach (P. Berardino, 2002) uses multiple small baseline (SB) acquisition subsets via an

Consequently, the DInSAR algorithm is moving from the conventional DInSAR technique to the study of the detected high coherent pixels (Usai, S. 2001), such as small man-made feature called Corner Reflector (CR) (Xia Y. 2002) and Permanent Scatters(PS) (A.Ferretti, 2001a,2000b), to generate deformation time-series that allows us to follow the evolution of the monitored deformations.

Conventional DInSAR approach has the limita

effective combination of all the available SB interferograms. The combination is based on a minimum-norm criterion of the velocity deformation via the application of the Singular Value Decomposition (SVD) method. The SBAS approach had two key advantages: (1) increased sampling rate by using all the acquisitions include in the SB subsets, and (2) preserved the capabilities of the system to provide spatially dense deformation maps, which being a key issue of conventional DInSAR interferometry (F. Casu, 2006).

This paper investigates SBAS approach; in particular, we assume a cubic behaviour for the time variation of the deformation phase signal as prior knowledge for the study area, the City of Nanjing, P. R. China, this simplified the SBAS method; 8 ERS2 SAR images acquired from 1996 to 2000 in descending orbit was used to demonstrate the capability of the simplified SBAS algorithm.

The paper is organized as follows: a short overview on the basic rationale of the SBAS algorithm is presented. Subsequently, we assume a cubic behaviour for the time variation of the deformation phase signal as prior knowledge to simplify the

---

* School of Civil Engineering Hohai University, No.1 Xikang Road, Nanjing, P.R.China;210098; Email: InSAR@hhu.edu.cn

SBAS approach. Then we focus on the results investigated by the simplified SBAS method in Nanjing, P. R. China. The last section is dedicated to the conclusion, summarizing the main findings in the paper.

2. DESCRIPTION OF THE SBAS-DINSAR ALGORITHM

A detailed discussion on the basic SBAS approach can be found in P. Bernardino (P. Berardino, 2002); accordingly, we highlight in this section what are the key issues of the algorithm.

Considering $N+1$ SAR images relative to the same area, acquired at the chronologically ordered times $(t_0, \cdots\cdots, t_N)$; assuming that each acquisition may be combined with at least one other image, also assuming that all the images are co-registered with respect to an image referred to as master one that allows us to identify a common spatial grid. The starting point of the SBAS technique is represented by the generation of a number, say M, of multilooked DInSAR interferograms that involves the previously mentioned set of $N+1$ SAR acquisitions. Note also that each of these interferograms should be calibrated with respect to a single pixel located in an area that can be assumed stable or, at least, with known deformation behaviour; this point is referred to as reference SAR pixel or reference point.

Now considering a generic pixel of azimuth and range coordinates (x, r); the expression of the generic j-th interferogram ($j = 1, \cdots\cdots, M$) computed from the SAR acquisitions at times t_A and t_B, will be the following (Tizzani P., 2007):

$$
\begin{aligned}
\delta\phi_j(x,r) &= \phi(t_B, x, r) - \phi(t_A, x, r) \\
&\approx \frac{4\pi}{\lambda}[d(t_B, x, r) - d(t_A, x, r)]
\end{aligned}
\tag{1}
$$

And

$$
\begin{aligned}
\phi(t_i, x, r) &= \frac{4\pi}{\lambda} d(t_i, x, r) \\
d(t_0, x, r) &= 0
\end{aligned}
$$

where λ is the radar wavelength, $\phi(t_i, x, r)$ is the unknown phase of the image involved in the interferogram generated between the time t_0 and t_i, $d(t_A, x, r)$ and $d(t_B, x, r)$ are the radar line of sight (LOS) projections of the cumulative surface deformation at the two times t_A and t_B.

In order to get a physically sound solution, replace the unknowns with the mean phase velocity between time-adjacent acquisitions, the new unknowns become:

$$
v^T = [v_1 = \frac{\phi_1}{t_1 - t_0}, \cdots\cdots, v_1 = \frac{\phi_N - \phi_{N-1}}{t_N - t_{N-1}}]
\tag{2}
$$

take (2) into (1):

$$
\sum_{k=IS_j+1}^{IE_j} (t_k - t_{k-1})v_k = \delta\phi_j
\tag{3}
$$

organized in a matrix form, finally leads to the expression

$$
Bv = \delta\phi
\tag{4}
$$

Note that in the equation (3) IE and IS corresponding to the acquisition time indexes associated with the image pairs used for the interferogram generation, note also that we assume the master (IE) and slave (IS) images to be chronologically ordered, i.e., $IE_j > IS_j, \forall j = 1, \cdots\cdots, M$, in the equation(4), B is $M \times N$ matrix. Of course, when solving the equation(4), the SVD decomposition is applied to the matrix B, and the minimum-norm constraint for the velocity vector v is applied in the final solution, to achieve the final solution ϕ, an additional integration step is necessary.

3. SBAS-DINSAR BASED ON PRIOR KNOWLEDGE

In fact, deformation in each image pixel has some relations between each acquisition, by including a mode for the phase behaviour, the above inverse problem can be simplified.

Assuming a linear relationship between the new model parameter vector p and the wanted velocity vector v:

$$
v = Mp
\tag{5}
$$

Where the columns of M describe the vector component of v, substituting this in(4) gives

$$
BMp = \delta\phi
\tag{6}
$$

A cubical model for the phase time variation can be written as:

$$\phi(t_i) = \overline{v}(t_i - t_0) + \frac{1}{2}\overline{a} \cdot (t_i - t_0)^2 + \frac{1}{6}\Delta\overline{a} \cdot (t_i - t_0)^3 \quad (7)$$

Where $\overline{v}$, $\overline{a}$ and $\Delta\overline{a}$ are the unknown mean velocity, mean acceleration, and mean acceleration variation respectively, the unknown model vector p in (6) is

$$p^T = [\overline{v}, \overline{a}, \Delta\overline{a}]^T \quad (8)$$

and the model matrix M is

$$M = \begin{bmatrix} 1 & \dfrac{t_1 - t_0}{2} & \dfrac{(t_1 - t_0)^2}{6} \\ 1 & \dfrac{t_2 + t_1 - 2t_0}{2} & \dfrac{(t_2 - t_0)^3 - (t_1 - t_0)^3}{6(t_2 - t_1)} \\ \cdots & \cdots & \cdots \\ 1 & \dfrac{t_N + t_{N-1} - 2t_0}{2} & \dfrac{(t_N - t_0)^3 - (t_{N-1} - t_0)^3}{6(t_N - t_{N-1})} \end{bmatrix}$$
$$(9)$$

By including this model, the equation system in (6) is generally simplified, for such a smooth temporal model, the product BM is nonsingular, the estimate of p can then be obtained by solving the following equation in an optimal LS way.

$$BMp + c \cdot \Delta h + \phi_A = \delta\phi \quad (10)$$

where $c \cdot \Delta h$ accounts for possible topographic artifacts due to error in the Digital Elevation Model (DEM) used for removal of the topographic phase , Δz is the DEM error, $c^T = [(4\pi/\lambda)(B_{\perp 1}/r\sin\upsilon), \cdots, (4\pi/\lambda)(B_{\perp M}/r\sin\upsilon)]$, $B_\perp$ is perpendicular baseline, r is sensor target distance, υ is look angle).

The key steps involved in the displacement time series retrieval implemented via the SBAS-DInSAR algorithm can be summarized as the follows:

1. Properly chosen the data pairs to generate the multilook DInSAR interferograms, the key objective of this step is to mitigate the decorrelation phenomena by introducing constraints on spatial baseline and temporal separation between the orbits relevant to interferometric SAR image couples.

2. Phase unwrapping of the original phase $\delta\phi_j(x,r)$, then calibrating them to a reference pixel as mentioned previously.

3. Assuming a relationship between the model parameter

vector and the phase velocity vector, then use the least square (LS) method to solve the equation(10).

4. The undesired atmosphere phase signal is detected as the result of the cascade of a low-pass filtering step, performed in the two-dimensional (2-D) spatial domain (i.e., azimuth and range), and a high-pass filtering operation with respect to the time variable.

4. RESULTS

A test site in the city Nanjing P. R. China has been chosen, see Fig. 1. Nanjing is the capital of Jiangsu Province, in an area surrounded to the west by the Yangtze River, to the east by Purple Mountain. New Qinhuai River in the south and the branches of Qinhuai River in the middle flow across the city from west to east, the west area of Qinhuai River is a new developed residential area which located in the stratum of the Yangtze River valley flat, where it is easily suffered from ground deformation.
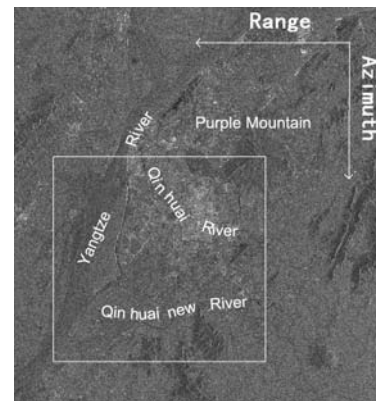

Fig. 1: City Nanjing in SAR amplitude image, the investigated area is highlighted

In order to validate the presented method, an ERS2 SAR data set composed by 8 acquisitions acquired from August 19,1996 until April 10,2000, on descending orbit, was first coregistered to the August 19,1996 scene, then we selected the combinations that exhibited a mutual perpendicular baseline less than 100m, and temporal baseline less than 4 years, this resulted in 2 different subsets, the 13 interferograms were generated by Doris software (Bert Kampes, 1999), characterize by a perpendicular baseline from 21.9m to 98.2m, temporal baseline from 35 days to 1158 days, in order to reduce the phase noise, a complex multi-look operation with 4 and 20 looks in range and azimuth, respectively, is carried out, the ground range pixel dimension of all products is therefore about 80×80m in the range and azimuth directions, respectively , see Table 1.The topographic component has been removed using a SRTM3 DEM, which has the height accuracy of about 16m (Bamler,1999), the ERS2 precise orbit state vector computed by the Technical University of Delft was used for flat earth reduction.

In order to exclude decorrelated areas from the study, we selected only the pixels that exhibited an estimated coherence value larger than 0.3, in at least 30%of the interferograms, based on the selected pixels, a Delauney triangulation was generated to connect these pixes, and interpolation was done for all the images in order to ease the phase unwrapping of the selected interferograms, see Fig. 2.

As far as phase unwrapping algorithm is concerned, the freely available phase unwrapping software called SNAPHU developed by Chen and Zebker (Chen C W, Zebker, 2001) have been chosen, after phase unwrapping, all pixels were calibrated with respect to an area that was assumed stable, the zero deformation value was taken as the mean of the phase values located within a 3*3 neighbourhood in an area with high coherence, in our case, the stable area was selected near to Purple Mountain which is in the north east of the study area, then, for each selected pixel, a joint estimation of DEM errors and the model parameter vector p is carried out by solving the equation(10) directly using the least square method.

No.	Master (y-m-d)	Slave (y-m-d)	$B_\perp$ (m)	$B_\parallel$ (m)	T(d)	Sub.
1	1999-10-18	1999-07-05	-98.2	39.9	105	1
2	1999-10-18	1999-04-26	-77.4	42.4	175	1
3	1999-10-18	1998-12-07	-48.8	23.1	315	1
4	1999-10-18	1996-08-19	-86.9	-3.0	1158	1
5	1999-07-05	1999-04-26	34.9	2.6	70	1
6	1999-07-05	1998-12-07	86.2	-16.8	210	1
7	1999-07-05	1996-08-19	21.9	-43.0	1050	1
8	1999-04-26	1998-12-07	53.2	-19.3	140	1
9	1999-04-26	1996-08-19	43.7	-45.6	980	1
10	1998-12-07	1996-08-19	-86.5	-26.1	840	1
11	2000-04-10	1997-12-22	-66.5	-118.9	840	2
12	2000-04-10	1997-11-17	-73.2	-80.3	875	2
13	1997-12-22	1997-11-17	-67.5	38.2	35	2

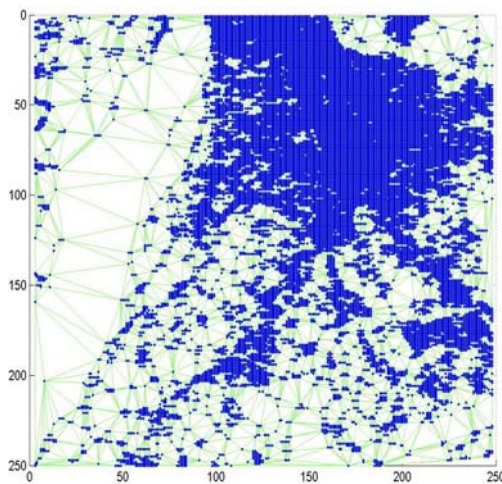Table 1: 13 interferograms generated by 8 ERS2 SAR images

Fig. 2: Generated Delauney triangulations

In order to provide an overall picture of the detected deformation, the false colour map representing the cumulative LOS deformation value for each investigated pixel was presented in Fig. 3, superimposed on the greyscale representation of the SAR image amplitude, areas where the measurements accuracy affected by decorrelation phenomena (coherence below the threshold) have been excluded from the false colour map, to be noted that, the image acquired on august 19,1996 was assumed as reference image with zero deformation,

and the reference point for each image used for phase calibration is marked with R.
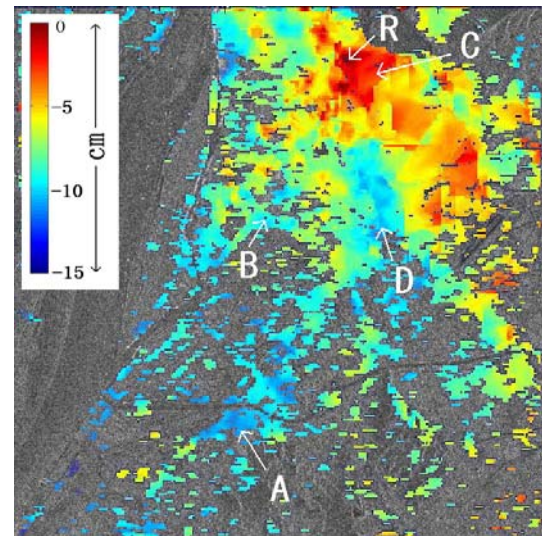

Fig. 3: LOS cumulative deformation maps superimposed on the SAR amplitude of the investigate area

Significant deformation is clearly shown in Fig. 3, it can be easily found that there are a large amount of sparsely distributed deformation pixels along the Yangtze River and the Qinhuai New River, most of the deformation areas are located in the west and south of the Qinhuai River, while in the north and east of the Qinhuai River, nearly no deformation was found; Another large deformation area is in the centre of the investigated area, which is on the alluvial floodplain of the ancient Qinhuai River, and now is the old city of the Nanjing. The largest deformation is 12.0cm, that the mean velocity of the subsidence is about 3.3cm/year, this agrees well with geodetic measurements carried out by some researchers.

In order to demonstrate the capability of the proposed approach to follow the temporal evolution of the detected deformation, some examples are provided in the following Fig. 4, presents the chronological sequence of the computed deformations for points (marked by A,B,C and D in Fig. 5) located in the area of maximum subsidence, except the point C which is near the reference point R, it can be seen that the observed deformations are characterized by a rather continuous subsidence phenomenon from 1996 until 2000, to be noted that, before the year 1999, all points of surface subsidence are small, in the image sequence of the December 7, 1998, even a amount of the increase in performance, subsidence become dramatically since the year 1999; it should be demonstrated whether this phenomenon has some relations with the Yangtze River water level change, particularly in the summer of 1998, the devastating floods of the Yangtze River lead to increased groundwater level.

From the above case study of ground deformation in Nanjing area, it can be seen that SBAS-DInSAR method have the following advantages: (1) Because of using small baseline subsets, this method has coherent area significantly larger than that of CR and PS method, not only to say traditional pointwise measurement such as GPS and levelling; (2) Ground control points is not necessary for SBAS-DInSAR method , (3) the use

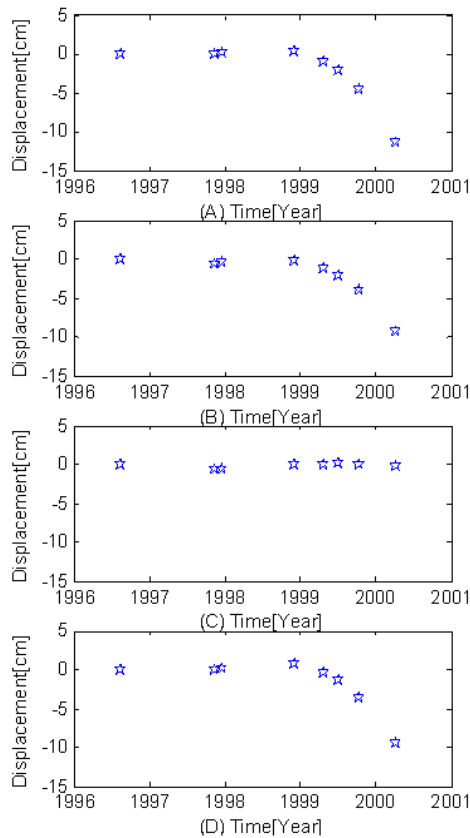earth observation methods is low cost, accessibility for large area deformation mapping.

Fig. 4: LOS displacement time series for the point A, B, C, D

5. CONCLUSIONS

This paper is focused on the investigation of the surface deformation of the city Nanjing, the over all analysis is based on the exploration of the SBAS-DInSAR approach with a prior deformation knowledge applied to a SAR data set acquired by the ERS-2 sensor during 1996-2000 time interval.

This study demonstrates the capability of the SBAS-DInSAR procedure to investigate the space-time characteristics of the deformation affecting the overall area. Moreover, we assume a cubic behaviour for the time variation of the deformation phase signal as a prior knowledge for the investigated area, and solve the equation in an optimal LS method directly, which simplify the SBAS-DInSAR algorithm. In particular, 13 interferograms in two subsets were generated using 8 ERS-2 SAR images acquired from August 1996 to April 2000 in Nanjing area, based on the cubic behaviour for the time variation of the deformation phase signal as prior knowledge, deformation map and displacement time series were generated using these 13 interferograms and the implemented SBAS-DInSAR algorithm.

Moreover, we find that the main deformation area is along the Yangtze River and to the west of the Qinhuai River, the maximum subsidence is around 12.0cm. finally, although the SAR images used in this study is relatively few, the deformation trend in the whole city has a good agreement with the conventional Leveling measurement, but more SAR images

should be used to get temporal behaviour of the deformation maps of the area, more sophisticate algorithm for detecting local deformations on a small spatial scale should be developed.

As an additional remark, the No. 1 north-south subway in Nanjing began in operation since September 2005. With a length of 21.72 km and 16 stations, Construction of the east-west No.2 subway with a length of 25.15 km is also in progress, developing new algorithm of InSAR technique to detect deformation along the subways is meaningful and challenge for the future.

REFERENCE

[1]. A.Ferretti, C.Prati, F.Rocca, "Permanent Scatters in SAR Interferometry," *IEEE Transactions on Geoscience and Remote Sensing*, Vol.39, No.1, January 2001

[2]. A.Ferretti, C.Prati, F.Rocca, "Nonlinear subsidence rate estimation using Permanent Scatters in Differential SAR Interferometry," *IEEE Transactions on Geoscience and Remote Sensing*, Vol.38, No.5, Sep. 2000

[3]. Bamler, Richard (1999): The SRTM Mission - A World-Wide 30 m Resolution DEM from SAR Interferometry in 11 Days. *Photogrammetric* Week 1999, S. 145~154, 47.

[4]. Bert Kampes, Delft Object-Oriented Radar *Interferometric Software: Users manual and technical documentation*, Delft University of Technology, Delft, 1.2 ed., 1999.

[5]. Chen C W, Zebker H A. Two-dimensional Phase Unwrapping with Use of Statistical Models for Cost Functions in Nonlinear Optimization. *Journal of the Optical Society of America A* , 2001 ,18(2) :338~351

[6]. C. Prati, F. Rocca, and A. Monti Guarnieri, "SAR interferometry experiments with ERS-1," in Proc. 1st ERS-1 Symp., Cannes, France, Nov. 4–6, 1992, pp. 211–218.

[7]. F. Casu, M. Manzo, R. Lanari. "A quantitative assessment of the SBAS algorithm performance for surface deformation retrieval from DInSAR data,". *Remote Sensing of Environment* 102 (2006) 195–210

[8]. P. Berardino, G. Fornaro, R. Lanari, and E. Sansosti, "A new algorithm for surface deformation monitoring based on small baseline differential interferograms," IEEE *Transactions on Geoscience and Remote Sensing*, Vol. 40, No. 11, 2375~2383, 2002.

[9]. Tizzani P., P. Berardino, F. Casu, P. Euillades, M. Manzo, G.P. Ricciardi, G. Zeni, R. Lanari (2007). Surface

deformation of Long Valley caldera and Mono Basin, California, investigated with the SBAS-InSAR approach. *Remote Sensing of Environment* 108 : 277-289.

[10]. Usai, S. A New Approach for Long Term Monitoring of Deformations by differential SAR Interferometry: [Ph. Doctor thesis]. Delft University, 2001

[11]. Xia Y., Kaufmann H. and Guo, X. F.: "Differential SAR Interferometry Using Corner Reflectors," IGARSS 2002, Toronto Canada, 24-28 June 2002, pp.1243-1246.